

# Adaptive Risk Tendency: Nano Drone Navigation in Cluttered Environments with Distributional Reinforcement Learning

Cheng Liu<sup>1</sup>, Erik-Jan van Kampen<sup>1</sup>, Guido C.H.E. de Croon<sup>1</sup>

**Abstract**—Enabling robots with the capability of assessing risk and making risk-aware decisions is widely considered a key step toward ensuring robustness for robots operating under uncertainty. In this paper, we consider the specific case of a nano drone robot learning to navigate an apriori unknown environment while avoiding obstacles under partial observability. We present a distributional reinforcement learning framework in order to learn adaptive risk tendency policies. Specifically, we propose to use tail conditional variance of the learnt action-value distribution as an uncertainty measurement, and use an exponentially weighted average forecasting algorithm to automatically adapt the risk-tendency at run-time based on the observed uncertainty in the environment. We show our algorithm can adjust its risk-sensitivity on the fly both in simulation and real-world experiments and achieving better performance than risk-neutral policy or risk-averse policies. Code and real-world experiment video can be found in this repository: <https://github.com/tudelft/risk-sensitive-rl.git>

## I. INTRODUCTION

Reinforcement learning (RL) is promising in solving sequential decision making problems such as robotic navigation with obstacle avoidance as it seeks the long-term optimal policy [1], [2]. Recent advances in deep reinforcement learning (DRL) which combine the power of deep neural networks with RL have shown the capability of achieving human-equal or even super human performance in diverse complex environments [3], [4], [5]. The majority of current deep RL methods are designed for maximizing the expectation of accumulated future returns, omitting to consider the risk of rare catastrophic events. However, when it comes to applying RL to safety-critical robots like drones, instead of aiming at achieving a high expected return, how to deal with risks and make decisions under uncertainty is crucial and still remains a challenge.

A natural way to make RL sensitive to risk is considering the worst-case of the stochastic return rather than its expectation, but this may lead to too conservative policies [6]. Recent works [7] proposed to model the distribution of the future return and generate multiple policies with different risk-sensitivities by changing levels of a risk measure. While [7] captures the stochasticity in accumulated returns by approximating the mean and variance of a Gaussian distribution, *distributional reinforcement learning* captures the randomness in accumulated returns by learning the true intrinsic distribution of future returns [8], [9], [10]. A major merit of distributional RL is that by giving different tendencies for risk, the learned policy can generate different



Fig. 1: A Crazyflie [13] nano drone navigating through a cluttered environment under partial observability.

actions with different level of cautiousness [11], [10], [12]. Distributional RL has been applied to some typical safety-critical applications such as autonomous driving at occluded intersections [14] and mobile-robot indoor navigation [15]. However, although these distributional RL based methods learn a policy that can vary its tendency for risk during training and adapt to multiple environments where different risk-sensitivities are required, humans are still needed to give the agent a level of tendency for risk for each environment before each deployment. A step towards building intelligent robots is developing the capability to adjusting the tendency for risk on the fly automatically. To achieve this goal, we propose the Adaptive Risk Tendency Implicit Quantile Network (ART-IQN) algorithm that can adapt its tendency for risk in a reactive way. We show the effectiveness of our algorithm in both simulation and real-world experiments on a safety-critical task - drone navigation with obstacle avoidance in cluttered environments (demonstrated in Fig. 1). ART-IQN showed superior performance in the trade-off between navigation efficiency and safety guarantee compared with risk-neutral and risk-averse baselines. Our main contributions are in three folds:

- A novel drone navigation algorithm based on distributional RL, that can learn a variety of risk-sensitive policies under partial observability;
- A dynamic adaption in tendency for risk on the fly based on uncertainty measure;
- A high-level sim-to-real reinforcement learning training framework that can generalize to real world scenarios without fine-tuning.

<sup>1</sup> Delft University of Technology, Email: c.liu-10@tudelft.nl, e.vankampen@tudelft.nl, g.c.h.e.decroon@tudelft.nl.

## II. RELATED WORK

### A. Risk and Uncertainty in Robot Navigation

RL-based robot navigation methods has gained momentum recently due to its robustness and a minimal requirement of manual engineering [16]. Several navigation algorithms based on RL also have emerged to address risks and uncertainties in the environment. [17] proposed to use a neural network to predict collision probability in future steps in obstacle avoidance tasks, and utilize MC-dropout [18] and bootstrapping [19] to estimate the uncertainty of the model prediction. Additionally, [20] enabled estimation of the regional increase of uncertainty in novel dynamic scenarios by introducing LSTM [21] to add memory of historical motion of the robot. [22] resorts to model-free policy network as action selector, has a GRU [23] to predict uncertainty in the local observation and uses the prediction variance to adjust the variance of the actions taken by the policy.

However, these methods either use MPC [24] as action selector which consumes a lot of computation resources and the Monte Carlo sampling even make it worse, or require an additional predictor model to estimate the uncertainty. In contrast, we use distributional RL as our framework, in this way, the risk measure and uncertainty estimation can be easily and efficiently implemented, which requires minimal additional computation resources.

### B. Distributional RL

An RL approach that has gained momentum recently is distributional RL, which proposes to take into account the whole distribution of value functions, rather than just the expectation [7], [8], [9], [10]. Since the whole distribution contains much more information beyond the first moment, one can leverage it to make more informed decisions that ultimately lead to superior rewards. Latest literature show that similar promising mechanisms also exist in human brains[25].

Two major concepts of distributional RL are distribution approximation and loss metric. The categorical DQN (CDQN) algorithm [8] use categorical distribution with fixed supports to approximate the probability density function (PDF) of the random return and use KL divergence as the loss metric between two approximated distributions. Another way to approximate the distribution is quantile regression. Compared to [8], the quantile regression DQN (QR-DQN) algorithm [9] learns the distribution by approximating the quantile function (QF) with fixed quantile values. The implicit quantile network (IQN) algorithm [10] improved the flexibility and accuracy of distribution approximation of [9] by learning these quantile values from quantile fractions sampled from a uniform distribution  $\mathcal{U}[0, 1]$ . This is achieved with a specific deep neural network representing the QF by mapping quantile fractions to quantile values with Wasserstein distance, a loss metric which indicates the minimal cost for transporting mass to make two distributions identical [10].

There has also been the application of distributional reinforcement learning to safety-critical environments. [14]

incorporates IQN to solve a autonomous driving task at intersections by combing risk-averse IQN with Safety guarantees. [15] proposes a method that an enable a mobile robot to navigate office scenarios with diverse risk-sensitivities.

Although the risk-sensitivity can be altered without re-training during deployment, all of those methods focus on applying distributional to safety-critical tasks which require human heuristics to define the risk tendency in advance. It is expected that fixing the risk-sensitivity level for the whole deployment episode is not optimal, since the risk of the trajectory is dynamic, and the agent should be able to react to a varying risk rather than simply following a fixed risk-tendency strategy. Our work require no heuristics about the deployment environment but let the agent adapt its risk tendency on its own.

The most related work to ours is [26], where the optimism and pessimism is dynamically chosen between different training episodes based on epistemic uncertainty [27] estimation. In our paper, we focus on adapting the tendency for risk after training where the aleatoric uncertainty [27] is the major concern.

## III. METHODOLOGY

### A. Problem Statement

1) *POMDP Setup*: An autonomous drone does not have full knowledge of the environment, but instead receives noisy partial observations from it. Therefore, the navigation problem can be formulated as a Partially Observable Markov Decision Process (POMDP) [28] in the RL framework. The POMDP can be defined as a tuple  $(\mathcal{S}, \mathcal{A}, \mathcal{O}, \mathcal{P}, R, \gamma)$ , where  $\mathcal{S}$ ,  $\mathcal{A}$  and  $\mathcal{O}$  represent the state, action and observation space. The drone interacts with the environment in discrete timesteps. At each timestep  $t$ , it receives the observation  $o_t \in \mathcal{O}$  from the environment and performs an action  $a_t \in \mathcal{A}$  based on its policy function  $\pi_t(a_t|o_t)$ , which causes a transition of the state from  $s_t$  to  $s_{t+1} \sim \mathcal{P}(\cdot|s_t, a_t)$ , and receives a reward  $r_t = R(s_t, a_t)$  and a new observation  $o_{t+1} \sim \mathcal{O}(\cdot|s_{t+1}, a_t)$ . Following policy  $\pi$ , the discounted sum of future rewards is denoted by the random variable  $Z^\pi(s_t, a_t) = \sum_{k=0}^{\infty} \gamma^k R(s_{t+k}, a_{t+k})$  with  $\gamma \in (0, 1)$  as the discount factor. Standard RL aims at maximizing the expectation of the discounted sum of future rewards, which is known as the action-value function  $Q^\pi(s_t, a_t) = \mathbb{E}[Z^\pi(s_t, a_t)]$ .

2) *States and Observations*: The state of the environment contains information about the drone itself, the goal and obstacles. Specifically, the state space describing state of the drone in the environment can be parameterized as  $s = (\mathbf{p}, d_g, \mathbf{d}_o)$ , where  $\mathbf{p}$  is the absolute drone position,  $d_g = \|\mathbf{p} - \mathbf{p}_g\|_2$  is the distance from the agent to goal point, and  $\mathbf{d}_o$  is a vector consisting of distances from the drone to surrounding obstacles.

For the drone itself, the state of the environment is not directly observable. Instead, the robot is equipped with sensors which provide partial observations to infer the state. We use Crazyflie, a 27.5g nano quadrotor as our real-world experiment platform. As shown in Fig. 2, the Crazyflie is equipped with four laser rangefinders in the drone's positive and

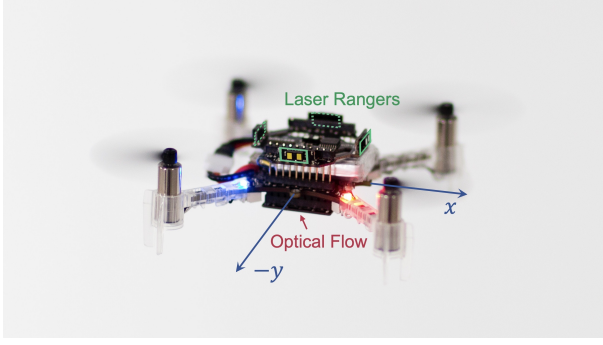


Fig. 2: A 27.5g Crazyflie nano drone with 4 laser rangefinders to detect obstacles and an optical flow camera to estimate velocity. [Picture by Guus Schoonewille, reprinted with permission of TU Delft]

negative  $x$  and  $y$  axis to detect and avoid obstacles. It also has an optical flow camera facing downwards to estimate its velocity for low-level flight control. The observation space of the drone can then be formulated as a tuple  $(\mathbf{p}, d_g, \mathbf{d}_r)$  where  $\mathbf{d}_r$  denotes the 4 laser reflections. The 4 laser rangefinders can detect obstacles with a maximum range of  $4m$ . In real experiments, The drone gets its absolute position observation and distance to the goal from OptiTrack, a 3D motion capturing system. The noise and uncertainty of this observation space mainly come from the partial observability of obstacles due to the fact that only obstacles that intersect with the laser beams will be detected.

3) *Action Space*: To incorporate with risk-sensitive policies, at each time step,  $a_t$  is designed to be a discretized command which gives the velocity magnitude and direction. The velocity magnitudes that can be chosen are  $k$  discretized values exponentially spaced in  $(0, v_{max}]$ . Since only obstacles that intersect with at least one of the 4 lasers will be detected, it will be reckless to move in directions that lasers not pointing especially when the obstacle is in a thin shape. As a consequence, there are 4 possible moving directions evenly spaced between  $[0, 2\pi)$ . In this paper,  $k = 3$  and  $v_{max} = 1$ , resulting in an action space with 12 discrete actions.

4) *Reward Function*: The reward function is designed to award the drone for reaching the goal as fast as possible, while penalizing for collisions or getting too close to obstacles:

$$R(s_t, a_t) = \begin{cases} 50 & d_g < 0.5 \\ 5(d_m - 0.2) & \text{radius} < d_m < d_d \\ -25 & d_m < \text{radius} \\ -0.1 & \text{otherwise,} \end{cases} \quad (1)$$

where  $d_m$  is the drone's distance to the closest obstacle,  $d_d$  is the safety margin distance, and radius represents the radius of the drone. Specifically, we set  $d_d = 0.2m$  and radius =  $0.05m$ .

## B. Adaptive Risk Tendency Implicit Quantile Network

To adjust the tendency for risk dynamically, we propose the *Adaptive Risk Tendency Implicit Quantile Network* (ART-IQN) algorithm. The main insight is that the most effective tendency for risk will not only vary across different environments, but also vary in even one deployment scenario. It is therefore sensible for an agent to adapt its level of risk-tendency dynamically in response to feedback from the environment on the fly.

1) *Implicit Quantile Network*: While standard RL aims at learning the expectation of the sum of discounted rewards, Distributional RL learns a value distribution of returns rather than the expected action-value. The distributional Bellman equation can be defined as

$$Z^\pi(s, a) \stackrel{D}{=} R(s, a) + \gamma Z(S', A'), \quad (2)$$

where  $\stackrel{D}{=}$  denotes equality in distribution, and the random variables  $S', A'$  are distributed according to  $S' \sim \mathcal{P}(s, a)$  and  $A' \sim \pi(\cdot | s')$ .

In particular, we represent the return distribution implicitly through its quantile function as in IQN algorithm [10]. This representation is used because many risk distortion operators can be efficiently computed using the quantile function of the underlying random variable. Concretely, we parameterize the quantile function through a neural network with learnable parameters  $\theta$ . We express such implicit quantile function as  $Z_\theta^\pi(s, a; \tau)$ , where  $\tau \in [0, 1]$  is the quantile level. To learn the parameters  $\theta$ , quantile regression is used, using a quantile Huber-loss as a surrogate of the Wasserstein-distance [10]. To this end, a target network with parameters  $\theta'$  is used and the temporal difference (TD) error at a sample  $(s, a, r, s')$  is computed as

$$\delta_{\tau, \tau'} = r + \gamma Z_{\theta'}^\pi(s', a'; \tau') - Z_\theta^\pi(s, a; \tau), \quad (3)$$

for  $\tau, \tau'$  independently sampled from the uniform distribution, i.e.  $\tau, \tau' \sim \mathcal{U}[0, 1]$  and  $a' \sim \pi(\cdot | s')$ . The  $\tau$ -quantile Huber-loss is

$$\rho_\kappa(\delta; \tau) = |\tau - \mathbb{I}\{\delta < 0\}| \frac{\mathcal{L}_\kappa(\delta)}{\kappa}, \text{ with } \mathcal{L}_\kappa(\delta) = \begin{cases} \frac{1}{2}\delta^2, & \text{if } |\delta| \leq \kappa \\ \kappa(|\delta| - \frac{1}{2}\kappa), & \text{otherwise,} \end{cases} \quad (4)$$

where  $\mathbb{I}$  is an indicator operator. Huber-loss  $\mathcal{L}_\kappa$  with threshold  $\kappa$  provides a smooth gradient-clipping here. Finally, we approximate the quantile loss for all levels  $\tau$  by sampling  $N$  independent quantiles  $\tau$  and  $N'$  independent target quantiles  $\tau'$ . The loss to update  $\theta$  is

$$\mathcal{L}(\theta) = \frac{1}{N \cdot N'} \sum_{i=1}^N \sum_{j=1}^{N'} \rho_\kappa(\delta_{\tau_i, \tau'_j}; \tau_i). \quad (5)$$

By backpropagating this loss function to  $\theta$ , we are minimizing the Wasserstein-distance between current action-value distribution and target action-value distribution as in Equation 2.

### 2) Risk-sensitive Policy and Conditional Value-at-Risk:

A distorted expectation is a risk weighted expectation of value distribution under a specific *distortion function* [12]. A distortion function indicates a non-decreasing function  $\beta : [0, 1] \rightarrow [0, 1]$  satisfying  $\beta(0) = 0$  and  $\beta(1) = 1$ . The distorted expectation of  $Z$  under  $\beta$  is defined as  $Q_\beta = \int_0^1 F_Z^{-1}(\tau) d\beta(\tau)$ , where  $F_Z^{-1}(\tau)$  is the quantile function or cumulative density function. According to [10], any distorted expectation can be represented as a weighted sum over the quantiles, then a corresponding sample-based risk-sensitive policy is obtained by approximating  $Q_\beta$  by  $K$  samples of  $\tilde{\tau} \sim \mathcal{U}[0, 1]$ :

$$\tilde{\pi}_\beta(s) = \arg \max_{a \in \mathcal{A}} \frac{1}{K} \sum_{k=1}^K Z_{\beta(\tilde{\tau}_k)}(s, a). \quad (6)$$

Changing the sampling distribution for  $\tau$  allows us to achieve various forms of risk-sensitive policies. Specifically, we consider Conditional Value-at-Risk (CVaR) [29], a *coherent risk measure* [6] as our distortion function. Its implementation as a modification to the sampling distribution of  $\tau$  is particularly simple, as it changes  $\tau \sim \mathcal{U}[0, 1]$  to  $\tau \sim \mathcal{U}[0, \alpha]$  by emphasizing the lower tail of the distribution as  $\alpha$  decreases to near zero and reduces to risk-neutral when  $\alpha = 1$ , where  $\alpha$  is the CVaR value. We choose CVaR to be our risk distortion function because: i) it's a coherent risk measure that can generalize to multiple return ranges; ii) it's relatively easy to combine with IQN by replacing the quantile sampling range; iii) by modifying CVaR value, it's effective and straightforward to show a diverse range of risk tendencies.

3) *Lower Tail Conditional Variance to Measure Uncertainty*: For a given action-value distribution in association with  $Z(s, a)$ , it's safe to say that the smaller its variance is, the more narrow the action-value is distributed, and less risk the mean of value distribution  $Q(s, a)$  can be used. It is then rational for an agent to adapt its tendency for risk dynamically in response to the variance of the value distribution. However, the distribution maybe asymmetric, which means the lower tail variability and the upper tail variability are not equal. Intuitively, for the sake of dealing with risk under uncertainty, lower tail is more biased towards negative rewards and is the part that we need to focus. Inspired by [30] where a decaying upper tail conditional variance of the return distribution is utilized for more efficient exploration during training, we use the lower tail conditional variance as an uncertainty measure for risk-tendency adaption. The lower half tail conditional variance is equivalent to the right truncated variance (RTV). Right truncation means dropping left part of the distribution with respect to the mean. Under the framework of IQN, calculation of RTV is straightforward:

$$RTV = \frac{1}{2N} \sum_{i=1}^{\frac{N}{2}} (\tau_i - \tau_{\frac{N}{2}})^2, \quad (7)$$

where  $\tau_i$  are the  $\frac{i}{N}$ -th quantile levels. Note that we calculate RTV with respect to the median rather than the mean due to

its statistical robustness [30], [31].

Since the deployment environment is an unknown prior to the drone, it is still not easy to evaluate the uncertainty from the absolute value of the tail conditional variance because it does not tell us about the relative risk level compared with other states. In other words, the truncated variance indicates the absolute uncertainty level in the environment at the current state, but does not tell us about relative uncertainty levels. In the next section, we show how we use the Exponentially Weighted Average Forecasting Algorithm (EWAF) [32] to utilize the relative uncertainty level between states to adapt the tendency for risks.

4) *Relative Uncertainty Level Forecasting for Risk Tendency Adaption*: Based on right truncated variance, we can get an estimation of the absolute level of uncertainties in the environment. But since the supports of the value distributions across states may be expansively different, it's not sensible to map the absolute uncertainty level to risk-tendency. Alternatively, we propose to use relative uncertainty changes between timesteps as our feedback to adapt the tendency for risk. Specifically, we firstly model the CVaR value as an output node from a softmax function with two logits. At each time step, we calculate the right truncated variance for current state-action pair, and then the weight of each softmax logit is updated according to the relative uncertainty changes.

Consider a softmax function with two weights  $w_1, w_2$ :  $\text{softmax}_i(w_i) = \exp(w_i) / \sum_i \exp(w_i), i = 1, 2$ . At each time step, the weights are updated, in accordance with the relative uncertainty change, by a learning rate  $\eta$ :

$$w_1 = w_1 - \eta \times f, w_2 = w_2 + \eta \times f, \quad (8)$$

where  $f = rtv_t - rtv_{t-1}$  is the feedback given by right truncated variance change at each timestep. Intuitively, a positive variance change indicates increasing uncertainty in the environment and a decreasing weight for softmax<sub>1</sub>. We define CVaR:  $\alpha = \text{softmax}_1$ , and to avoid  $\alpha$  approaching zero, at each time step an additional logit exponential weight  $\sum_i \exp(w_i)/b$  is added both to the sum of logits and CVaR exponential weights, which results in a CVaR range of  $(\frac{1}{b+1}, 1)$ . Here  $b = 9$  is chosen, so  $\alpha \in (0.1, 1)$ . Now we get the ART-IQN algorithm that can adapt its tendency for risk implemented by CVaR value dynamic choosing strategy. Intuitively, if the right truncated variance of the value distribution is increasing and the current risk-sensitivity is low, the tendency of being more risk-averse will increase, which in our case is choosing smaller  $\alpha$  to sample actions.

## IV. RESULTS

### A. Simulation Experiments

1) *Environment*: We design a OpenAI gym [33] like environment provided with the given state and observation space as give in section III-A.2. We assume the velocity command could be immediately executed at each time step without delays and the time step is set to be 0.1s. We use domain randomization [34] to train a policy that can deal with different scenarios, which is, the obstacle density, shape

TABLE I: Quantitative Evaluation Results

Density	CVaR	Success rate	Collision rate	Navigation time
2	0.10	0.87	<b>0.09</b>	06.41
2	0.25	<b>0.88</b>	0.10	06.31
2	0.50	0.87	0.11	05.30
2	0.75	0.84	0.13	05.25
2	1.00	0.86	0.12	<b>05.12</b>
2	ART-IQN	0.87	0.11	05.32
6	0.10	0.74	<b>0.15</b>	12.52
6	0.25	<b>0.77</b>	0.17	10.23
6	0.50	0.72	0.19	08.46
6	0.75	0.69	0.22	08.57
6	1.00	0.67	0.30	<b>07.89</b>
6	ART-IQN	0.74	0.17	08.26
12	0.10	0.64	0.21	18.52
12	0.25	0.67	0.25	13.23
12	0.50	0.66	0.28	09.46
12	0.75	0.62	0.31	08.60
12	1.00	0.57	0.41	<b>08.05</b>
12	ART-IQN	<b>0.70</b>	<b>0.15</b>	11.76

and position are all randomly sampled at the start of each training episode. In the real world, the lasers exhibit noise, in that they do not detect the distance to obstacles perfectly. As a consequence, Gaussian noise  $\mathcal{N}(\mu, \sigma)$  with mean  $\mu = 0.0$  and standard deviation  $\sigma = 0.01$  is added to the measurement of each laser ranger. A noise value is sampled independently for each ranger. After adding noise, the resulting range is clipped to lie between the sensor's minimum and maximum ranges, which is  $[0, 4]m$ .

2) *Training Process*: The model is trained following curriculum learning where the complexity of environment is increased as the training process goes on. The first stage of training uses an environment with a randomized goal distance  $d_g \in [2, 3]$  meters and a randomized number of square and wall shaped obstacles  $n_{obs} \in [0, 5]$ , where  $n_{obs}$  is the number of obstacles. After training a number of episodes (until a success rate of 0.8 is reached), the complexity of the environment is increased by adding more obstacles to the environment, which will be then be  $n_{obs} \in [6, 12]$ . The whole training process takes a total of 3.5 hours and achieves a final success rate of 0.88. To make sure our algorithm experiences a diverse range of trajectories under a variety of policies with different risk tendencies, at each training episode, the CVaR value is also uniformly sampled with  $\alpha \sim \mathcal{U}(0, 1]$ .

The neural network we used has 3 hidden layers, each layer is a fully connected layer with 512 units. Each fully-connected layer is followed with ReLU [35] activation function except the output layer. Adam [36] is used as the optimizer with learning rate  $5 \times 10^{-4}$  and batch size 64. An update is performed for every 5 episodes, the discount factor  $\gamma$  is set to be 0.99. An episode is terminated after 25 seconds without reaching the goal or collision.

3) *Evaluations*: To show the effectiveness of our algorithm, ART-IQN is evaluated with both risk-neutral IQN and IQN with multiple risk tendency levels with  $\alpha = 0.1, 0.25, 0.5, 0.75$ . Note that a risk-neutral IQN equals to  $\alpha = 1.0$ . Since IQN only uses risk-sensitivity to adjust its policy, but not its value distribution, the risk-sensitivity of the policy can be tuned using  $\alpha$  at execution time without

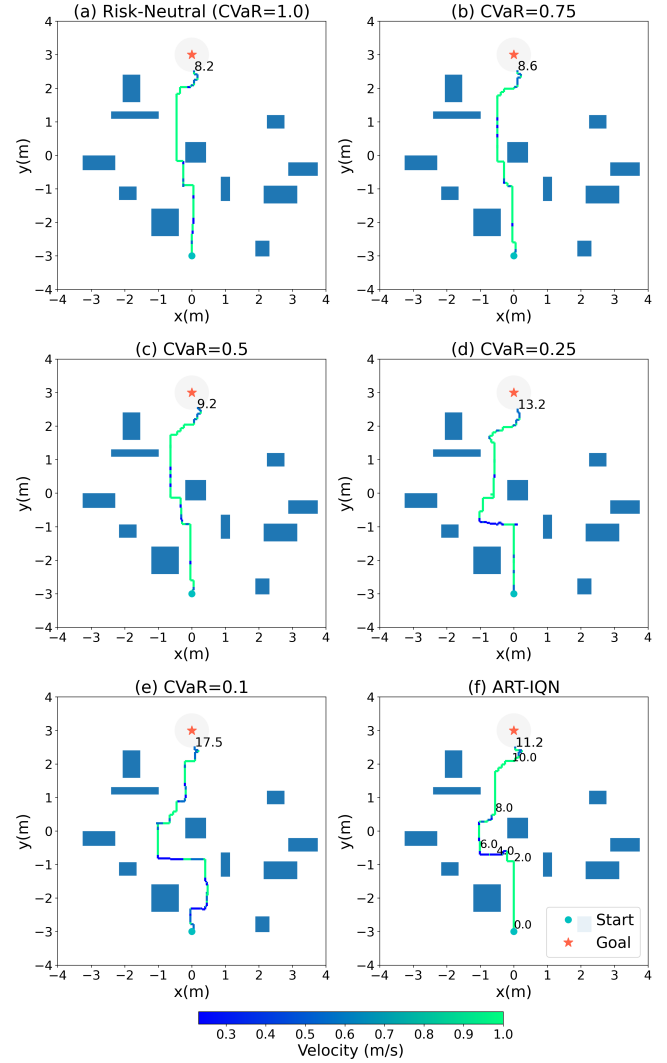


Fig. 3: Drone behavior demonstration and task finishing time comparison with different risk-sensitivities. While the risk-neutral policy can fulfill the task in the shortest time, it gets too close to the obstacles by ignoring the risk in the environment. Risk-averse policies with smaller CVaR values can generate safer policies but sacrifice in navigation efficiency. Our ART-IQN algorithm can balance this efficiency-safety trade-off by dynamically choosing risk tendency according to the uncertainty estimation.

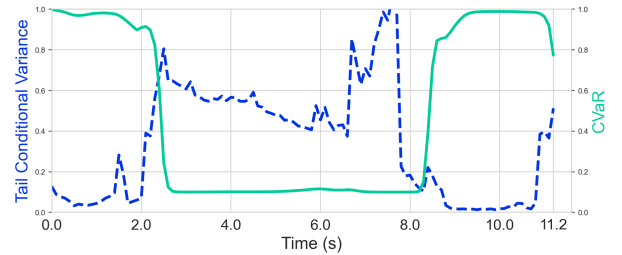


Fig. 4: Right truncated tail conditional variance and adaptive CVaR of ART-IQN. It can be seen that ART-IQN can adapt its CVaR value to different lower tail conditional variance levels as an estimation of uncertainty in the environment.

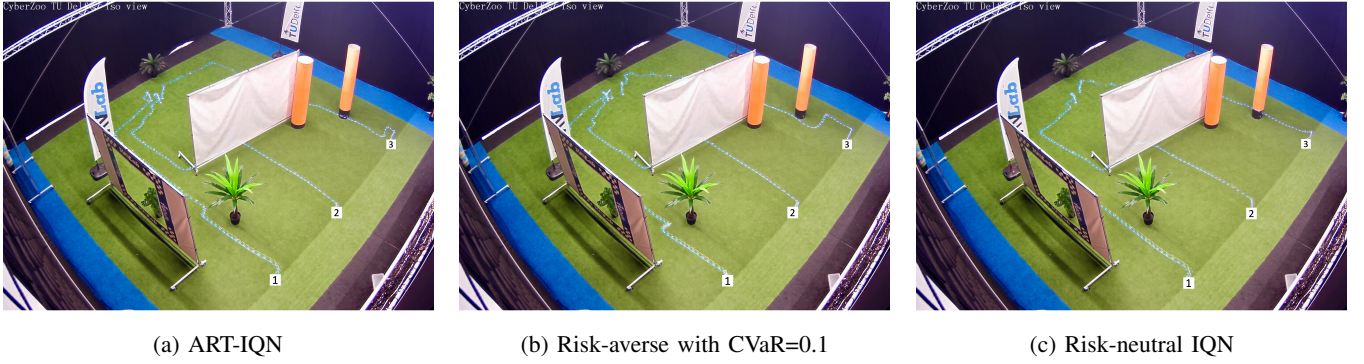


Fig. 5: Image frames for real-world experiments. The trajectory is plotted with the blue LED on the drone. Additional real-world experiment video can be found in <https://github.com/tudelft/risk-sensitive-rl.git>.

requiring retraining of the policy for different risk levels. The average navigation time, collision rates and episode scores are compared across different random environments. Specifically, the evaluation is executed on environments with three different obstacle densities 2, 6, 12, and 100 runs for each density. To ensure fairness and reproducibility, fixed random seeds are used for evaluations under the same density, so different CVaR are evaluated on exactly the same sequences of randomly generated environments, with fixed starting and random goal positions in  $[0, d_g]$  where  $d_g$  is sampled from  $\mathcal{U}[2, 3]$ .

Table I gives a quantitative result comparing ART-IQN and IQN with different risk tendencies. For density 2, it can be seen that ART-IQN and IQN with multiple CVaR values can finish the navigation task at a high success rate and a low collision rate since the environment is easy. For density 6, while IQN with low CVaR values can maintain a low collision rate compared with high CVaR values, the task finishing time is long and the chance for timeout increases too. In contrast, ART-IQN can still achieve a high success rate while maintain a low collision rate, and finish the task in a decent time. for density 12, the success rate for all CVaR values including ART-IQN decrease obviously due to the difficulty of the task. However, while low CVaR values run into more cases of timeout and high CVaR values encounter more collision, ART-IQN can achieve the best in success rate and collision rate, while maintain a moderate task finishing time.

We show the qualitative evaluation results in Fig. 3 by giving a typical environment encountered during evaluation. A risk-neutral policy would choose actions that have higher averaged returns as shown in Fig. 3 (a) with CVaR=1.0 to achieve the goal as fast as possible, yet it ignores the risk from getting too close to obstacles which lead to higher rates of collisions. Although the risk-neutral policy has higher average returns, it is not aware of the uncertainty or the risk in this task framework due to the partial observability, which is reflected in the higher collision rates and aggressive manners. On the other hand, risk-averse policies, especially the one with  $\alpha = 0.1$  as show in Fig. 3 (e), keep a safe distance to obstacles but lead to conservative policies that

will increase the task finishing time. In comparison, ART-IQN can finish the task in an adaptive manner, which is trying to avoid obstacles cautiously in the middle area of environment where there is more uncertainty encountered, and to achieve a higher speed when it's more certain about the its current state as shown in Fig. 3 (f).

Fig. 4 shows the corresponding right truncated tail conditional variance in the trajectory from Fig. 3 (f). At the start of the episode, the drone starts with  $\alpha = 1.0$  and flies at speed of  $v = 1.0m/s$ , which is risk-neutral since it does not know the environment yet. During 0 to 2.0 seconds, the tendency for risk is near risk-neutral as the uncertainty is relatively low. Around 2.0 to 8.0 seconds, the truncated increases and keeps at a high level, which resulted a decrease in CVaR values, and the drone shows a risk-averse manner to keep distance to obstacles and fly at a lower speed. From 8.0 until the end of this episode, the estimated uncertainty decreases fast and keeps at a low level, CVaR also decreases accordingly and resulted a risk-neutral risk tendency. It is clear that as the drone navigate through the environment, it senses a variance changing pattern and adjusts its risk tendency, represented by CVaR values, and results in a policy to be risk-averse when the uncertainty increases substantially and risk-neutral when the uncertainty is low.

## B. Real-World Experiments

We also do real-world experiments in a motion capture enabled  $5m \times 5m$  environment using a crazyflie nano drone. The nano drone we used is shown in Fig. 2, has dimensions  $92 \times 92 \times 29mm$  and weighs 27.5 grams. We put reflective markers on the four propellers to let the motion capture system track its position. All action selection using the learned policies is performed on a laptop, and the communication with the Crazyflie is done via a radio-to-USB dongle. The command frequency is set to be the same as in simulation, which is 0.1s. For the cluttered environment, as shown in Fig. 5, we put tree-like, gate-like obstacles and cylinders in the environment that the agent has never seen in the simulation. We test CVaR=0.1, CVaR=1.0 and ART-IQN for a comparison. Each agent is initialized in the environment

at 3 different locations for 3 runs, resulted a total number of 27 runs. All the runs succeeded except the Risk-neutral IQN when its initialized in the left. For Risk-neutral IQN, the drone collides with the flag on the left corner due to its fast speed and can not avoid it in time. Comparing trajectory 2 in Fig. 5, the risk-neutral agent also gets too close to the white board and reacts to it in a delay. For trajectory 3, the ART-IQN and risk-averse policy with CVaR=0.1 can both detect the cylinder obstacle in advance and find a path through, while risk-neutral policy nearly ignores the cylinder and fly past it in such a short distance.

## V. CONCLUSION

In conclusion, focusing on the drone navigation with obstacle avoidance task under partial observability, we propose a novel adaptive risk tendency distributional reinforcement learning algorithm to adapt risk tendency to the estimated uncertainty in the environment. Our algorithm uses exponential weight forecasting to adjust risk tendency represented by the CVaR risk measure, with lower tail conditional variance as an measure of the uncertainty. We show the effectiveness of our algorithm both in simulation and real-world experimental environments. Results show that our algorithm can achieve higher task finishing efficiency while keeping the collision rate low.

The main drawback of our method is that during evaluation in environments with high obstacle density, ART-IQN encounters a obvious decrease in performance. The possible reason for this is the severe partial observability of the system due to the fact that i) only four lasers are used and ii) we are relying only on the current observation with no memory used. Future work can be focused on improving the robustness of the system by introducing recurrent networks or increasing the observation reliability, for example by equipping cameras on the drone. Besides, the uncertainty to risk tendency inference is rather intuitive, although it can work in our setting, tuning the learning rate for weight forecasting still requires human effort. This part can be improved by enabling the agent to learn this inference by itself.

## ACKNOWLEDGMENT

The authors would like to thank Jinke He for the wonderful discussions and Bart Duisterhof, Yingfu Xu for the real-world experiment setup.

## REFERENCES

- [1] R. S. Sutton and A. G. Barto, *Reinforcement Learning: An Introduction*, 2nd ed. The MIT Press, 2018. [Online]. Available: <http://incompleteideas.net/book/the-book-2nd.html>
- [2] C. Watkins and P. Dayan, "Q-learning," *Machine Learning*, vol. 8, no. 3/4, pp. 279–292, 1992.
- [3] V. Mnih, K. Kavukcuoglu, D. Silver, A. A. Rusu, J. Veness, M. G. Bellemare, A. Graves, M. Riedmiller, A. K. Fidjeland, G. Ostrovski, S. Petersen, C. Beattie, A. Sadik, I. Antonoglou, H. King, D. Kumaran, D. Wierstra, S. Legg, and D. Hassabis, "Human-level control through deep reinforcement learning," *Nature*, vol. 518, no. 7540, pp. 529–533, Feb. 2015. [Online]. Available: <http://dx.doi.org/10.1038/nature14236>
- [4] T. P. Lillicrap, J. J. Hunt, A. Pritzel, N. Heess, T. Erez, Y. Tassa, D. Silver, and D. Wierstra, "Continuous control with deep reinforcement learning," in *4th International Conference on Learning Representations, ICLR, 2016*. [Online]. Available: <http://dblp.uni-trier.de/db/conf/iclr/iclr2016.html#LillicrapHPHETS15>
- [5] S. Levine, C. Finn, T. Darrell, and P. Abbeel, "End-to-end training of deep visuomotor policies," *J. Mach. Learn. Res.*, vol. 17, pp. 39:1–39:40, 2016. [Online]. Available: <http://jmlr.org/papers/v17/15-522.html>
- [6] A. Majumdar and M. Pavone, "How should a robot assess risk? towards an axiomatic theory of risk in robotics," *CoRR*, vol. abs/1710.11040, 2017. [Online]. Available: <http://arxiv.org/abs/1710.11040>
- [7] Y. C. Tang, J. Zhang, and R. Salakhutdinov, "Worst cases policy gradients," in *3rd Annual Conference on Robot Learning, CoRL 2019, Osaka, Japan, October 30 - November 1, 2019, Proceedings*, ser. Proceedings of Machine Learning Research, L. P. Kaelbling, D. Kragic, and K. Sugiura, Eds., vol. 100. PMLR, 2019, pp. 1078–1093. [Online]. Available: <http://proceedings.mlr.press/v100/tang20a.html>
- [8] M. G. Bellemare, W. Dabney, and R. Munos, "A distributional perspective on reinforcement learning," in *Proceedings of the 34th International Conference on Machine Learning, ICML 2017, Sydney, NSW, Australia, 6-11 August 2017*, ser. Proceedings of Machine Learning Research, D. Precup and Y. W. Teh, Eds., vol. 70. PMLR, 2017, pp. 449–458. [Online]. Available: <http://proceedings.mlr.press/v70/bellemare17a.html>
- [9] W. Dabney, M. Rowland, M. G. Bellemare, and R. Munos, "Distributional reinforcement learning with quantile regression," *CoRR*, vol. abs/1710.10044, 2017. [Online]. Available: <http://arxiv.org/abs/1710.10044>
- [10] W. Dabney, G. Ostrovski, D. Silver, and R. Munos, "Implicit quantile networks for distributional reinforcement learning," in *Proceedings of the 35th International Conference on Machine Learning, ICML 2018, Stockholm, Sweden, July 10-15, 2018*, ser. Proceedings of Machine Learning Research, J. G. Dy and A. Krause, Eds., vol. 80. PMLR, 2018, pp. 1104–1113. [Online]. Available: <http://proceedings.mlr.press/v80/dabney18a.html>
- [11] N. A. Urpi, S. Curi, and A. Krause, "Risk-averse offline reinforcement learning," *CoRR*, vol. abs/2102.05371, 2021. [Online]. Available: <https://arxiv.org/abs/2102.05371>
- [12] X. Ma, Q. Zhang, L. Xia, Z. Zhou, J. Yang, and Q. Zhao, "Distributional soft actor critic for risk sensitive learning," *CoRR*, vol. abs/2004.14547, 2020. [Online]. Available: <https://arxiv.org/abs/2004.14547>
- [13] bitcraze, *Crazyflie 2.1 Specifications*. [Online]. Available: <https://www.bitcraze.io/products/crazyflie-2-1/>
- [14] D. Kamran, T. Engelgeh, M. Busch, J. Fischer, and C. Stiller, "Minimizing safety interference for safe and comfortable automated driving with distributional reinforcement learning," in *IEEE/RSJ International Conference on Intelligent Robots and Systems, IROS 2021, Prague, Czech Republic, September 27 - Oct. 1, 2021*. IEEE, 2021, pp. 1236–1243. [Online]. Available: <https://doi.org/10.1109/IROS51168.2021.9636847>
- [15] J. Choi, C. R. Dance, J. Kim, S. Hwang, and K. Park, "Risk-conditioned distributional soft actor-critic for risk-sensitive navigation," in *IEEE International Conference on Robotics and Automation, ICRA 2021, Xi'an, China, May 30 - June 5, 2021*. IEEE, 2021, pp. 8337–8344. [Online]. Available: <https://doi.org/10.1109/ICRA48506.2021.9560962>
- [16] V. Francois-Lavet, P. Henderson, R. Islam, M. G. Bellemare, and J. Pineau, "An introduction to deep reinforcement learning," 2018, cite arxiv:1811.12560. [Online]. Available: <http://arxiv.org/abs/1811.12560>
- [17] G. Kahn, A. Villafior, V. Pong, P. Abbeel, and S. Levine, "Uncertainty-aware reinforcement learning for collision avoidance," *CoRR*, vol. abs/1702.01182, 2017. [Online]. Available: <http://arxiv.org/abs/1702.01182>
- [18] Y. Gal and Z. Ghahramani, "Dropout as a bayesian approximation: Representing model uncertainty in deep learning," in *Proceedings of the 33rd International Conference on Machine Learning, ICML 2016, New York City, NY, USA, June 19-24, 2016*, ser. JMLR Workshop and Conference Proceedings, M. Balcan and K. Q. Weinberger, Eds., vol. 48. JMLR.org, 2016, pp. 1050–1059. [Online]. Available: <http://proceedings.mlr.press/v48/gal16.html>
- [19] I. Osband, C. Blundell, A. Pritzel, and B. V. Roy, "Deep exploration

- via bootstrapped DQN,” in *Advances in Neural Information Processing Systems 29: Annual Conference on Neural Information Processing Systems 2016, December 5-10, 2016, Barcelona, Spain*, D. D. Lee, M. Sugiyama, U. von Luxburg, I. Guyon, and R. Garnett, Eds., 2016, pp. 4026–4034. [Online]. Available: <https://proceedings.neurips.cc/paper/2016/hash/8d8818c8e140c64c743113f563cf750f-Abstract.html>
- [20] B. Lütjens, M. Everett, and J. P. How, “Safe reinforcement learning with model uncertainty estimates,” in *International Conference on Robotics and Automation, ICRA 2019, Montreal, QC, Canada, May 20-24, 2019*. IEEE, 2019, pp. 8662–8668. [Online]. Available: <https://doi.org/10.1109/ICRA.2019.8793611>
- [21] S. Hochreiter and J. Schmidhuber, “Long short-term memory,” *Neural computation*, vol. 9, pp. 1735–80, 12 1997.
- [22] T. Fan, P. Long, W. Liu, J. Pan, R. Yang, and D. Manocha, “Learning resilient behaviors for navigation under uncertainty,” in *2020 IEEE International Conference on Robotics and Automation, ICRA 2020, Paris, France, May 31 - August 31, 2020*. IEEE, 2020, pp. 5299–5305. [Online]. Available: <https://doi.org/10.1109/ICRA40945.2020.9196785>
- [23] K. Cho, B. van Merriënboer, D. Bahdanau, and Y. Bengio, “On the properties of neural machine translation: Encoder-decoder approaches,” *CoRR*, vol. abs/1409.1259, 2014. [Online]. Available: <http://arxiv.org/abs/1409.1259>
- [24] E. F. Camacho and C. B. Alba, *Model predictive control*. Springer science & business media, 2013.
- [25] W. Dabney, Z. Kurth-Nelson, N. Uchida, C. K. Starkweather, D. Hassabis, R. Munos, and M. Botvinick, “A distributional code for value in dopamine-based reinforcement learning,” *Nat.*, vol. 577, no. 7792, pp. 671–675, 2020. [Online]. Available: <https://doi.org/10.1038/s41586-019-1924-6>
- [26] T. Moskovitz, J. Parker-Holder, A. Pacchiano, and M. Arbel, “Deep reinforcement learning with dynamic optimism,” *CoRR*, vol. abs/2102.03765, 2021. [Online]. Available: <https://arxiv.org/abs/2102.03765>
- [27] W. R. Clements, B. Robaglia, B. V. Delft, R. B. Slaoui, and S. Toth, “Estimating risk and uncertainty in deep reinforcement learning,” *CoRR*, vol. abs/1905.09638, 2019. [Online]. Available: <http://arxiv.org/abs/1905.09638>
- [28] M. T. Spaan, “Partially observable markov decision processes,” in *Reinforcement Learning*. Springer, 2012, pp. 387–414.
- [29] C. Filippi, G. Guastaroba, and M. G. Speranza, “Conditional value-at-risk beyond finance: a survey,” *Int. Trans. Oper. Res.*, vol. 27, no. 3, pp. 1277–1319, 2020. [Online]. Available: <https://doi.org/10.1111/itor.12726>
- [30] B. Mavrin, H. Yao, L. Kong, K. Wu, and Y. Yu, “Distributional reinforcement learning for efficient exploration,” in *Proceedings of the 36th International Conference on Machine Learning, ICML 2019, 9-15 June 2019, Long Beach, California, USA*, ser. Proceedings of Machine Learning Research, K. Chaudhuri and R. Salakhutdinov, Eds., vol. 97. PMLR, 2019, pp. 4424–4434. [Online]. Available: <http://proceedings.mlr.press/v97/mavrin19a.html>
- [31] P. Huber, J. Wiley, and W. InterScience, *Robust statistics*. Wiley New York, 1981.
- [32] N. Cesa-Bianchi and G. Lugosi, *Prediction, learning, and games*. Cambridge University Press, 2006.
- [33] OpenAI, *OpenAI gym environments*. [Online]. Available: [https://gym.openai.com/envs/#classic\\_control](https://gym.openai.com/envs/#classic_control)
- [34] J. Tobin, R. Fong, A. Ray, J. Schneider, W. Zaremba, and P. Abbeel, “Domain randomization for transferring deep neural networks from simulation to the real world,” in *2017 IEEE/RSJ International Conference on Intelligent Robots and Systems (IROS)*, 2017, pp. 23–30.
- [35] A. F. Agarap, “Deep learning using rectified linear units (relu),” *ArXiv*, vol. abs/1803.08375, 2018.
- [36] D. P. Kingma and J. Ba, “Adam: A method for stochastic optimization,” in *3rd International Conference on Learning Representations, ICLR 2015, San Diego, CA, USA, May 7-9, 2015, Conference Track Proceedings*, 2015. [Online]. Available: <http://arxiv.org/abs/1412.6980>